Spectator Detection for the Measurement of Proton-Neutron Interactions at ANKE

I. Lehmann [a,b,1], S. Barsov [c], R. Schleichert [a], C. Wilkin [d],
M. Drochner [e], M. Hartmann [a], V. Hejny [a], S. Merzliakov [f],
S. Mikirtychiants [c], A. Mussgiller [a], D. Protić [a], H. Ströher [a],
S. Trusov [g,b], P. Wüstner [e]

[a]*Institut für Kernphysik, Forschungszentrum Jülich, D-52425 Jülich, Germany*

[b]*Institut für Kern und Hadronenphysik, Forschungszentrum Rossendorf,
D-01314 Dresden, Germany*

[c]*High Energy Physics Department, Petersburg Nuclear Physics Institute,
188350 Gatchina, Russia*

[d]*Physics & Astronomy Department, UCL, Gower Street, London WC1E 6BT, UK*

[e]*Zentralinstitut für Elektronik, Forschungszentrum Jülich, D-52425 Jülich,
Germany*

[f]*Laboratory of Nuclear Problems, Joint Institute for Nuclear Research, Dubna,
141980 Dubna, Russia*

[g]*Skobeltsin Institute for Nuclear Physics of M. V. Lomonosov Moscow State
University, Vorobjovy Gory, 119899 Moscow, Russia*

Abstract

A telescope of three silicon detectors has been installed close to the internal target position of the ANKE spectrometer, which is situated inside the ultra-high vacuum of the COSY-Jülich light-ion storage ring. The detection and identification of slow protons and deuterons emerging from a deuterium cluster-jet target thus becomes feasible. A good measurement of the energy and angle of such a *spectator* proton (p_{sp}) allows one to identify a reaction as having taken place on the neutron in the target and then to determine the kinematical variables of the ion-neutron system on an event-by-event basis over a range of c.m. energies.

The system has been successfully tested under laboratory conditions. By measuring the spectator proton in the $pd \to p_{sp} d\pi^0$ reaction in coincidence with a fast deuteron in the ANKE Forward Detector, values of the $pn \to d\pi^0$ total cross section have been deduced. Further applications of the telescope include the determination of the luminosity and beam polarisation which are required for several experiments.

Key words: Proton-neutron quasi-free interactions, Proton spectator detection, Position sensitive silicon telescope

PACS: 25.40.Fq, 25.40.Ca, 29.40.Wk, 29.20.-c

1 Introduction

In any thorough investigation of meson production or other reactions resulting from nucleon-nucleon collisions, it is important to have proton-neutron data as well as proton-proton. Medium energy neutron beams, even when produced from stripped deuterons, have a significant momentum spread. Unless the np centre-of-mass energy is determined by other means, such as by measuring all final-state particles, these neutron beams are not suitable for measuring cross sections that vary fast with energy, as is the case for meson production near threshold. The alternative, of using the neutron inside deuterium as a target for a proton beam, faces similar problems due to the Fermi motion of the neutron in the target. Despite the typical neutron momentum in the deuteron being only around 60 MeV/c, this spreads the c.m. energy by approximately 100 MeV, depending upon the mass of the meson being produced. A precise experiment therefore requires all final-state particles to be measured also in this approach.

The suggestion of using the deuteron as a substitute for a neutron target is very plausible because the average proton-neutron separation in the nucleus is about 4 fm, which is large compared to the typical range of forces between elementary particles. To a good first approximation then, an incident particle will interact with either a proton or neutron target, leaving the other nucleon in the deuteron as a *spectator*, moving with the momentum that it had before the collision. In the thick targets used in bubble chamber or electronic measurements with external beams, one rarely detects such a spectator particle, which has an energy of only a few MeV. This situation has been radically changed with the advent of medium energy proton storage rings where one can work with thin windowless targets. It then becomes feasible to measure the proton spectators in solid state counters placed in the vacuum of the target chamber inside such a ring. Knowing the beam energy and the spectator momentum allows one to reconstruct the c.m. energy of the proton-neutron system without measuring all the particles produced in this reaction. In this way it is possible to exploit the intrinsic target momenta, measuring a cross section over a range of well-defined c.m. energies while working at a fixed beam momentum. Furthermore, merely identifying a spectator proton p_{sp} is an indication that the production reaction has taken place on the neutron and not on the proton, thus simplifying significantly the subsequent data analysis.

These ideas have all been successfully tested in an initial experiment at the CELSIUS ring, where the spectator protons were measured in a set of sim-

Email address: `r.schleichert@fz-juelich.de` (R. Schleichert).
[1] Current address: Department of Radiation Sciences, University of Uppsala, Box 535, S-75121 Uppsala, Sweden

ple silicon detectors [1]. All final particles in the $pd \rightarrow p_{\text{sp}}d\pi^0$ reaction were detected, with the two photons from the π^0 decay being used as the trigger. Using a circulating beam whose energy was fixed at 320 MeV, the authors could deduce within the spectator model the variation of the $pn \rightarrow d\pi^0$ total cross section at five c.m. energies near threshold and this agreed with the results from standard data compilations. On the other hand, the lack of an independent luminosity measurement meant that it was not possible to determine absolute cross sections. Since there is no room for these spectator counters in the new WASA target chamber at CELSIUS, they are now being used at COSY to study the $pn \rightarrow pn\eta'$ reaction [2].

At the COSY-ANKE facility of the Forschungszentrum Jülich we have extended the CELSIUS technique by constructing a telescope of three silicon detectors, the details of which are given in section 2. The self-triggering capabilities of the telescope allow efficient data taking at high particle fluxes. As discussed in the following section, the set-up yields good measurements of both the energies and angles of slow protons and deuterons emerging from a deuterium target. Using the E-ΔE technique the system permits particle identification and, in particular, the separation of recoil protons from deuterons over significant energy ranges. One new feature of this set-up is its capability of working down to proton momenta of $70\,\text{MeV/c}$. Not only are the achievable statistics significantly increased, as compared to experiments with higher threshold energies, but also the interpretation of the data in terms of its model dependence becomes substantially simplified.

The technique is put to the test in section 4, where the measurement of the $pd \rightarrow p_{\text{sp}}d\pi^0$ reaction away from threshold is described. By using a deuterium cluster-jet target and detecting the fast deuteron in the forward system of the ANKE magnetic spectrometer, the π^0 could be identified as a peak in the $p_{\text{sp}}d$ missing mass. The $pn \rightarrow d\pi^0$ total cross section thus extracted agrees with the results deduced from previous experiments.

In subsequent experiments the spectator telescope has been used to measure the total cross sections for the $pn \rightarrow d\omega$ [3,4] and $pn \rightarrow d\eta$ [5] reactions near threshold. At the high beam momenta required for ω production, the recoil deuterons from elastic proton-deuteron scattering can also be detected in the telescope and used to determine the luminosity by comparing with known $pd \rightarrow pd$ differential cross sections. Another application of the set-up is the measurement of the beam polarisation, which is vitally important for the polarised experimental programme at ANKE. These measurements, and the outlook for further work, are outlined in our conclusions of the final section.

2 Silicon Telescope

The ANKE facility is a magnetic spectrometer and detection system placed at an internal target position of the COSY light-ion storage ring [6]. In order to extend its capabilities through the detection of recoil particles with very low momenta, a telescope consisting of three layers of silicon detectors has been chosen, as sketched in top view in Fig. 1. This enables tracking, energy determination, and particle identification to be carried out within the constraints imposed by the restricted space inside the ANKE vacuum chamber.
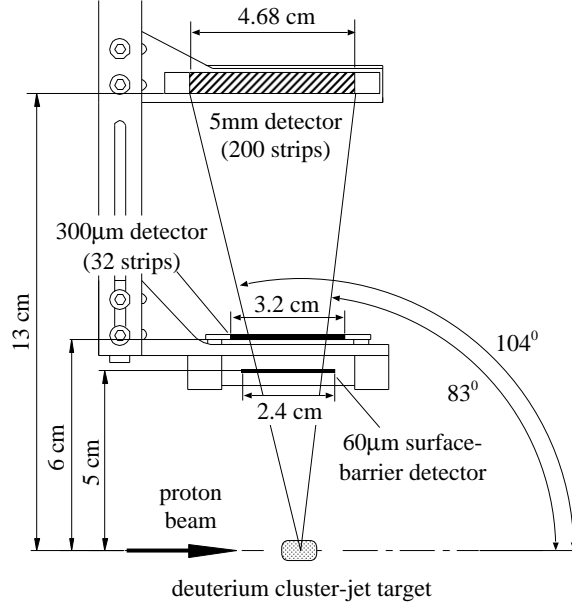

Fig. 1. Sketch of top view of the silicon telescope inside the ANKE target chamber showing the COSY beam, the cluster target and the telescope structure of three silicon detectors.

In order to identify a particle *via* the E-ΔE method and to determine its kinetic energy, it has to be stopped after traversing a preceding detector and depositing part of its energy therein. Now the Fermi momentum of a spectator proton in the deuteron is on average about $60 \, \text{MeV/c}$ ($T_p \approx 1.9 \, \text{MeV}$) and only about 5% of protons have momenta above $250 \, \text{MeV/c}$. Moreover, at the higher momenta one has problems in being sure that the recoil proton is indeed a spectator rather than an active participant in a reaction.

A $5 \, \text{mm}$ thick lithium-drifted strip detector [7] stops protons with kinetic energies up to $31 \, \text{MeV}$, *i.e.* momenta up to $250 \, \text{MeV/c}$. Taken in combination with a $300 \, \mu\text{m}$ thick detector, protons with $T_p \geq 6.7 \, \text{MeV}$ could in principle be used. However, as will be seen in the following section, detection thresholds and angular straggling considerations increase this limit to $8 \, \text{MeV}$. In order to extend this range down to kinetic energies of $2.5 \, \text{MeV}$, an initial layer con-

sisting of a $60\,\mu$m thick surface-barrier detector was also installed. This choice combines a low threshold for protons, with energy deposits sufficient to distinguish protons from deuterons. Though it would have been very helpful to reduce the energy threshold for spectator protons by using, say, an $18\,\mu$m thick surface-barrier detector, it was found in a separate test measurement [8] that the energy resolution *versus* band separation in this case would not suffice to distinguish between protons and deuterons. The details of the layers finally chosen are given in Table 1.

Table 1
Principal properties of the detectors used in the spectator telescope. The first layer is circular and not segmented. For the others, the number of strips and their pitch, is given. The energy resolution of the detectors was deduced from measurements with an α-particle source, and the full-width at half maximum (FWHM) of the peaks, which characterises the noise level, is given.

	1st layer	2nd layer	3rd layer
Silicon detector type	Surface barrier	Implanted	Lithium-drifted
Sensitive thickness	$60.9\,\mu$m	$306\,\mu$m	$5.1\,$mm
Entrance window [Si-eqv.]	$0.08\,\mu$m	$\leq 1.5\,\mu$m	$\leq 1\,\mu$m
Exit window [Si-eqv.]	$0.23\,\mu$m	$\leq 1.5\,\mu$m	$\leq 1\,$mm
Active area	$450\,$mm^2	$32 \times 15\,$mm^2	$47 \times 23\,$mm^2
Segmentation	1	32	200
Pitch	—	$1\,$mm	$235\,\mu$m
Noise	$100\,$keV	$70\,$keV	$80\,$keV

With respect to the incident beam direction, angles from the deuterium cluster-jet target between 83 and 104° are covered in the horizontal plane, whereas in the vertical direction limits of $\pm10°$ and $\pm7°$ are set by the second and third layers respectively. Having some coverage in the forward hemisphere is important because deuterons from elastic proton-deuteron scattering, used for luminosity determination at high energies as well as for the alignment, cannot go backwards in the laboratory frame.

Simple kinematic arguments show that, for counters placed close to 90°, both the c.m. energy W_{pn} of the proton-neutron system and the typical missing-mass determinations depend even more sensitively upon the polar angle of the spectator proton than on its energy. To handle this, the second and third layers of the telescope are composed of strips arranged perpendicularly to the beam. The surface-barrier detector and all 32 strips of the $300\,\mu$m thick detector are read out individually using analogue electronics. Preamplifiers with a gain of

55 mV/MeV are placed outside the vacuum about 10 cm from the detectors. The shaper amplifiers, with shaping constants of $1\,\mu$s differentiating and $1\,\mu$s integrating, are placed 20 m apart. The latter 32 channels have additionally been equipped with fast shaper amplifiers (shaping constants: $1\,\mu$s differentiating, 10 ns integrating) and discriminators to allow triggering. This feature is essential for efficient data-taking at high particle fluxes because the elastic and quasi-free elastic channels cannot be efficiently suppressed by the on-line trigger from the ANKE forward system alone. The last layer, however, has been equipped with 4 resistor chains such that 8 read-out channels are sufficient to obtain the energy loss and coordinate, using the sum and difference of amplitudes respectively [8,9]. Due to the higher dynamic range, the gain of the preamplifiers is only 5 mV/MeV with an unchanged shaping constant of $1\,\mu$s of the main amplifieres. The angular resolution that can be obtained with the chosen arrangement will be discussed in the next section.

One big advantage of our set-up is that it allows us to determine the relative positions of the target and detectors far more accurately than can be done by conventional techniques. This is because the elastic proton-deuteron kinematics are fully determined by the measurement of the deuteron kinetic energy in the second and third layers of the telescope. For this reason an accurate energy calibration of the system was performed, as described below. With the achieved precision of 1% in the particle's kinetic energy, the telescope could be aligned to within a few tenths of a millimetre with respect to the target. Moreover, the angles of the ANKE forward system could also be determined with respect to the target and beam to about 0.05°. Though this feature is useful when determining the spectator angles, it is essential for reliable acceptance calculations.

The amplitudes for each read-out channel were calibrated individually using α-particle sources in combination with an electronic pulser designed to deliver precise attenuation factors. Taken together with the known energy deposit from the α-particles, an absolute calibration was then obtained including all the non-linearities of the system, as shown e.g. for the second layer by Fig. 2(a). The pulser amplitudes have been calibrated simultaneously, allowing them to be used to calibrate the complete system at any time after their installation at COSY. In order to monitor the calibration of the 300 μm and 5 mm thick detectors simultaneously with the measurements, two low-intensity α-particle sources (50 and 500 Bq) were permanently mounted in the system. The strengths were such that, while being negligible compared to the primary count rate, more than 300 events could be collected per read-out channel within a typical run-time of two hours. These yielded clean peaks above the background, as shown in Fig. 2(b).
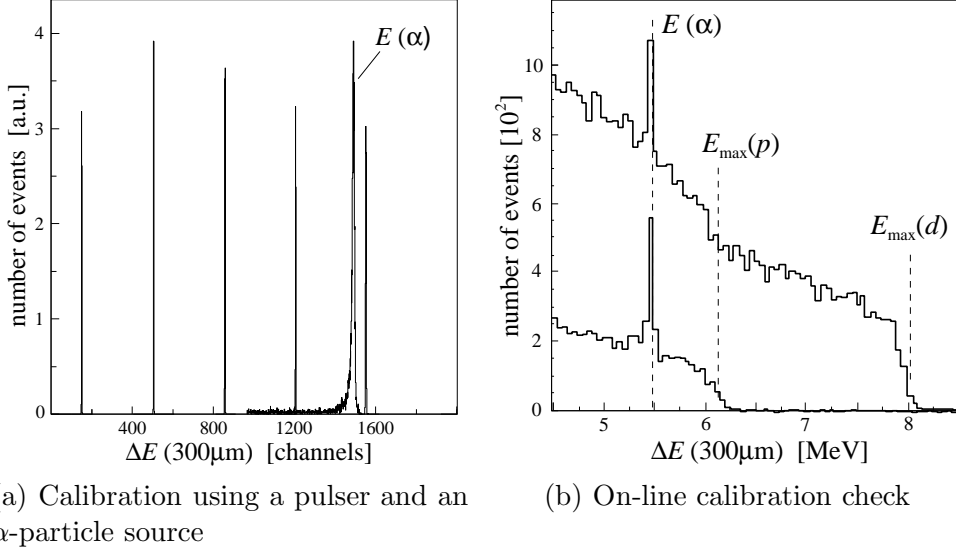
6

(a) Calibration using a pulser and an α-particle source

(b) On-line calibration check

Fig. 2. Laboratory calibration and on-line check for the second telescope layer. (a) The pulser signals and α-peak position permit an absolute off-line calibration. The calibration at the accelerator can be achieved using the calibrated pulser signals and cross-checked by the experimental data shown in (b). The upper distribution was obtained by selecting forward angles, where elastically scattered deuterons are present, whereas only protons can contribute in the backward hemisphere shown in the lower distribution. The absolute energy calibration was controlled by the well-defined energy loss of stopped α-particles coming from permanently mounted sources $E(\alpha)$ (narrow peaks) and by the maximum energy loss for protons and deuterons, $E_{max}(p)$ and $E_{max}(d)$ respectively.

3   Spectator Proton Detection

Particle identification is carried out using the E-ΔE technique, as illustrated in Fig. 3. The agreement between the experimental data and the predicted proton and deuteron curves for the two pairs of counters prove that the systematic error in the absolute kinetic energy determination is below 1%.

To quantify the background arising from possible misidentification, slices have been cut from Fig. 3 and the resulting projections plotted in Fig. 4. The effective resolution, including all experimental contributions such as straggling, detector and electronic response, *etc.*, was found to be such that the bands are separated over our full range by more than two and six times their widths for the low and high energy particles respectively. From this it is already clear that, by applying an appropriate cut between the bands, protons can be well separated from deuterons. The residual deuteron background becomes completely insignificant if elastic events are further suppressed by information from the ANKE forward system, as shown by the dashed histograms in Fig. 4.

7
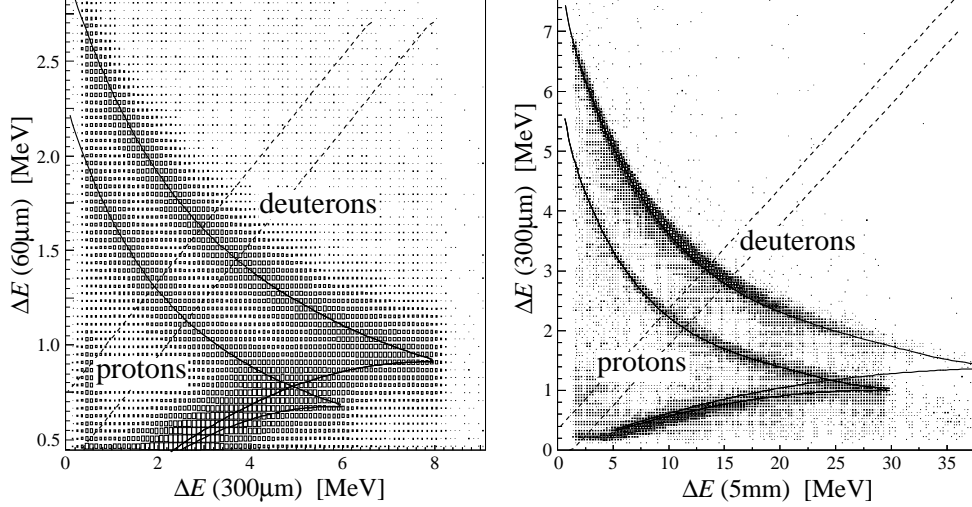
(a) Energy losses in the $60\,\mu$m *versus* $300\,\mu$m silicon detectors

(b) Energy losses in the $300\,\mu$m *versus* 5 mm silicon detectors

Fig. 3. Particle identification achieved by comparing energy deposits in two layers of the telescope. The boxes represent experimental data whereas the curves correspond to the predicted energy losses of protons and deuterons in silicon [10]. The deuteron band in (b), obtained at 2.8 GeV/c, largely disappears at low beam momenta due to the restricted geometrical acceptance of the system; the recoil deuterons from elastic pd scattering then generally have too little energy. The cuts applied to produce Figures 4 are indicated by the dashed lines.

The energy range of the telescope divides naturally into the two classes of events shown in Figs. 3(a),(b). Protons with kinetic energies between 2.3 and 6.7 MeV traverse the $60\,\mu$m surface-barrier detector and stop in the second layer whereas those that stop in the final layer have energies up to 31 MeV. The identification of protons by the E-ΔE method is, however, complicated in the transition region between these two ranges. As shown in Fig. 3(a), the band arising from deuterons traversing the first two layers, but missing the third, overlaps with that from stopped protons. Taking into account the finite energy resolution, protons are only completely distinguished from deuterons in the low energy range of Fig. 3(a) for $T_p < 4.4$ MeV. On the other hand, the lower limit that we have taken for the second range, $T_p > 8$ MeV, has been set by the straggling considerations discussed below. The overlap of the deuteron band imposes no restriction since deuterons with energies above ≈ 30 MeV are not scattered into the acceptance of the system.
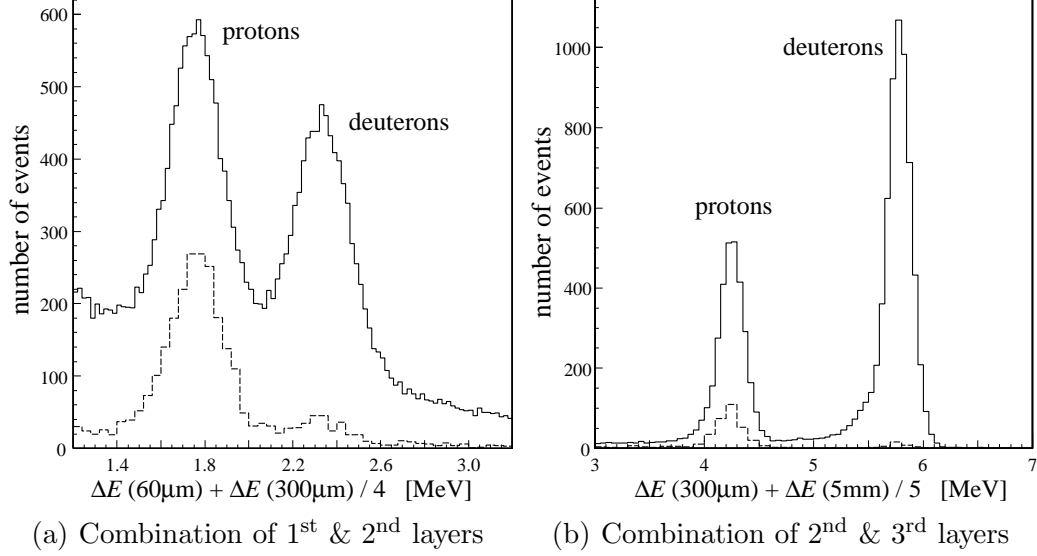
(a) Combination of 1st & 2nd layers   (b) Combination of 2nd & 3rd layers

Fig. 4. Projections of the slices in the E-ΔE spectra obtained by applying the cuts indicated by the dashed lines in Figs. 3. These correspond to the combinations $\Delta E(60\,\mu\text{m}) + \Delta E(300\,\mu\text{m})/4$ and $\Delta E(300\,\mu\text{m}) + \Delta E(5\,\text{mm})/5$ respectively. The solid histograms, scaled by factors of 0.2 and 0.05 for (a) and (b) respectively, show the separation of the proton and deuteron bands in both energy ranges. The dashed histograms are obtained after the rejection of elastic events on the basis of information obtained from the forward system.

The $60\,\mu\text{m}$ layer has no spatial resolution but the $300\,\mu\text{m}$ and $5\,\text{mm}$ detectors each have strips on one of their sides. These are placed perpendicular to the beam direction, leading to a purely geometrical angular resolution $\sigma(\theta)$ of about $0.4°$ in the horizontal plane. Now, within our geometry, the polar angle can be well approximated by this horizontal angle. However, even for the relatively fast deuterons used to measure the luminosity and relative alignment to the target, straggling of more than $1°$ dominates the resolution. The angle of the protons from the lower energy range, where the only position information is provided by the strip number in the second layer, is determined using the relative position of the target centre. The finite target size then fixes the spectator polar angle to within $\pm 5°$. There remains an acceptable background of a few per cent of events not originating from the target. For the higher energy protons we have chosen a lower limit of $8\,\text{MeV}$ in order to limit the straggling to be below $3°$. The vertical angle is fixed only by the target and detector sizes but this corresponds essentially to the azimuthal angle, which has no influence on the determination of the c.m. energy. The characteristics of the two detection ranges are summarised in Table 2.

Table 2
Effective ranges of detection, angular resolution and band separation in terms of FWHM in the silicon telescope

Combination	1st & 2nd	2nd & 3rd
T_p-range	$2.6 - 4.4\,\text{MeV}$	$8 - 22\,\text{MeV}$
p_p-range	$70 - 91\,\text{MeV/c}$	$123 - 204\,\text{MeV/c}$
$\sigma(\theta_p)$	$\approx 5°$	$\leq 3°$
Band separation	$> 2 \times \text{FWHM}$	$> 6 \times \text{FWHM}$

In order to study the experimental energy and angular resolution of the silicon layers *prior* to the measurements at COSY, a dedicated experiment was performed using the proton beam at the Tandem Accelerator of the Institute of Nuclear Physics of the University of Cologne [8]. This led to the choice of a suitable first layer detector. It also showed that the position in the 5 mm detector, read out using a resistor chain, could be reconstructed with an accuracy better than $300\,\mu\text{m}$ in absolute value. The angular resolution is then dominated by angular straggling, which was measured to be in good agreement with results from Monte-Carlo simulations [11].

The target chamber of ANKE is placed just in front of the spectrometer magnet D2 such that the low energy protons and deuterons detected by the telescope are perturbed by the stray magnetic field. Though the fields in this region, $B \lesssim 0.1\,\text{T}$, are much smaller than the maximum values in the spectrometer, $B = 1.6\,\text{T}$, significant corrections have to be introduced because of the low spectator proton momenta. Corrections of $0.6°$ to $1.8°$ relative to straight lines, depending upon the spectator energy, have been obtained from Monte Carlo simulations [11].

4 Measurement of the $pd \to p_{sp}d\pi^0$ Reaction

The magnetic dipole of ANKE, combined with the forward detector system of multiwire proportional counters (MWPCs), scintillator hodoscope and inclined Čerenkov counters, allows us to identify and measure the momenta of fast particles produced in coincidence with spectator protons in the silicon telescope. This system, illustrated in Fig. 5, is described in detail in Ref. [6]. The detection and identification of two charged particles allows one to select the production of a single meson, such as the π^0, η, or ω, through the missing mass technique.
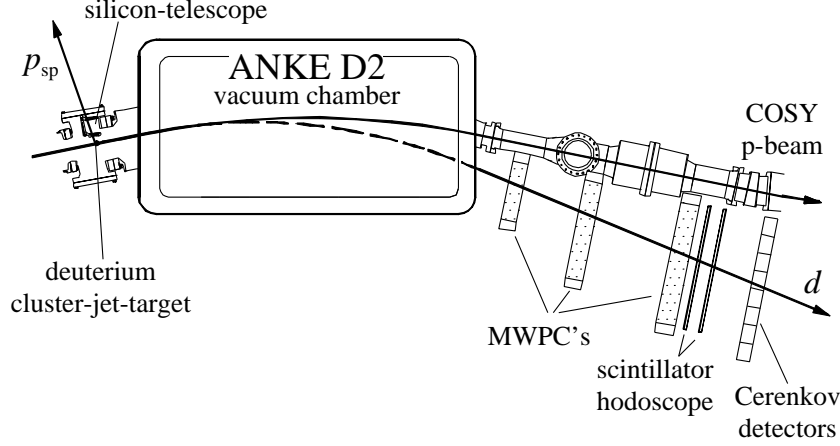
Fig. 5. The part of the ANKE set-up used for the measurement of the $pd \rightarrow p_{\mathrm{sp}}d\pi^0$ reaction. Sketched are the circulating COSY proton beam, the target chamber with the telescope for spectator proton detection, the vacuum chamber of the spectrometer dipole magnet D2, and the forward detection system used to track and identify fast deuterons.
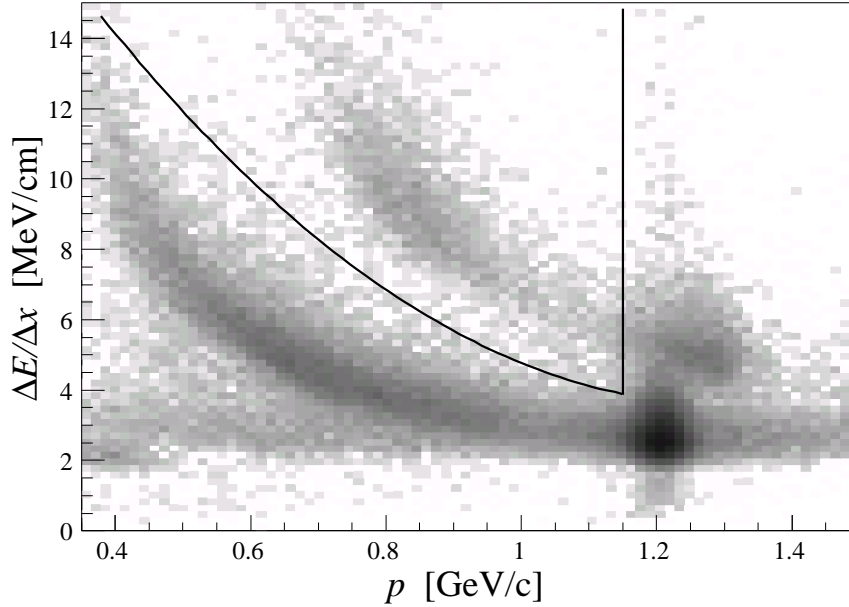

Fig. 6. The normalised energy loss per centimetre for particles in the first hodoscope layer of the ANKE forward detector *versus* their measured momentum. Clearly visible are the upper and lower bands originating from deuterons and protons respectively. Note that the statistics for protons are orders of magnitude greater than for deuterons. The lines indicate the cuts applied to select deuterons shown in Fig. 7(a)

To test this method of investigating meson production in proton-neutron interactions at ANKE, we have measured the $pd \rightarrow p_{\mathrm{sp}}d\pi^0$ reaction at a beam momentum of $1.2\,\mathrm{GeV/c}$. In Fig. 6 the energy losses of particles in the first plane of the scintillator hodoscope of ANKE are plotted *versus* their reconstructed

11

momenta. The spectrum is dominated by the proton peak around $1.2\,\mathrm{GeV/c}$ corresponding to small-angle deuteron break-up events. However, one also observes clear proton and deuteron bands and, by imposing a momentum-dependent threshold between them, one can reduce the proton contribution significantly. Since the Landau tail from the quasi-elastic protons cannot be suppressed very effectively at high momenta, only the range below $1.15\,\mathrm{GeV/c}$ was selected when extracting the $pn \to d\pi^0$ cross section, as indicated in Fig. 6.

The experimental momentum distribution is compared in Fig. 7(a) to a Gaussian fit for the $d\pi^0$ events plus a polynomial *ansatz* for the background. The number of detected events for the $pn \to d\pi^0$ reaction has been deduced solely from this figure where, unlike for the missing-mass representation, the distribution is not biased by the assumption that the fast particle is a deuteron. Since the experiment was carried out very close to the two-pion threshold, the background must arise primarily from protons misidentified as deuterons. This is consistent with the missing mass distribution for the same events, which is shown in Fig. 7(b). There is a clear peak at around $140\,\mathrm{MeV/c^2}$, corresponding to the undetected π^0. The large width comes from measuring pion production well above threshold with a limited angular resolution of the forward array. The small shift compared to the true pion mass is consistent with the geometric precision of the set-up. The second peak towards the maximum missing mass is due to the proton background.
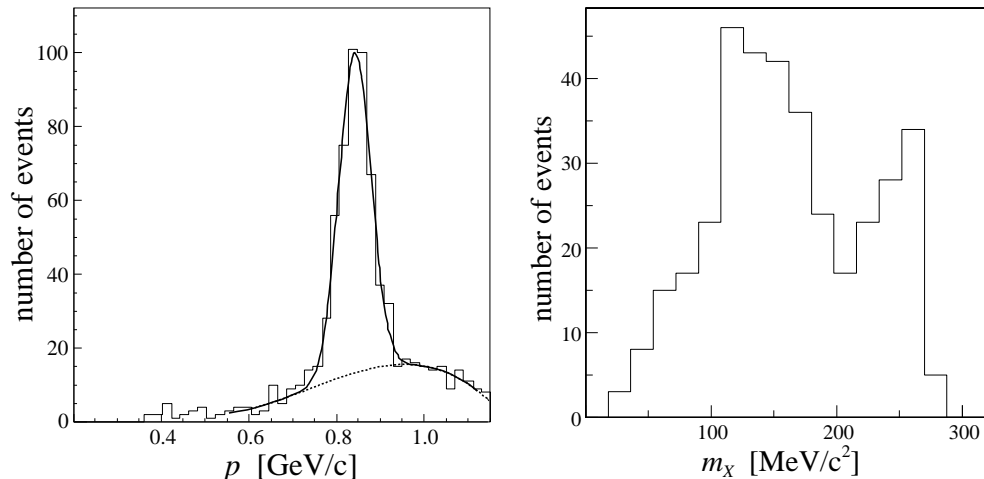
(a) Deuteron momentum distribution using the cuts indicated in Fig. 6

(b) Missing mass distribution for the events in (a)

Fig. 7. Momentum and missing mass distributions using spectator protons with $2.6 \le T_{\mathrm{sp}} \le 4.4\,\mathrm{MeV}$ and energy losses in the hodoscope for proton suppression.

The integrated luminosity for the π^0 production experiment at $600\,\mathrm{MeV}$ was obtained by counting protons elastically and quasi-elastically scattered from the target at laboratory angles between $5°$ and $10°$, as described in Ref. [12].

It is not possible to separate cleanly $pd \to pd$ from $pd \to ppn$ events using just the ANKE Forward Detector information, though the momentum resolution is sufficient to exclude pion production. The inclusive pd differential cross section can be reliably estimated within the Glauber model [13]. Such a calculation, which takes into account the sum of elastic and inelastic terms in closure approximation, could be checked in part using the results obtained on the $pd \to pd$ differential cross section, which has been measured close to our energy at $T_p = (582 \pm 10)$ MeV [14]. It is believed that the luminosity can be obtained to $\pm 7\%$ using this procedure [15]. The reduction in flux due to the presence of a second nucleon in the target (shadowing), has been taken into account by a 5% correction, similar to that used for η production [16].

To calculate the acceptance of the whole system, the $pd \to p_{\rm sp} d\pi^0$ reaction was simulated using the PLUTO event generator [17], which includes the Fermi motion in the deuteron. The events thus obtained were fed into the standard GEANT3 program [11], adjusted to the geometry of the ANKE. Finally, the momenta of both the spectator proton and fast deuteron were subjected to the experimental cuts imposed by the spectator telescope and forward detector system respectively.

After correcting for the tracking efficiency in the wire chambers and the spectator detection, we deduce a total cross section of $\sigma_{\rm tot}(pn \to d\pi^0) = (1.62 \pm 0.14)$ mb at an effective mean beam energy of $T_{\rm beam} = 556$ MeV. The c.m. energy is here reconstructd to 7 MeV FWHM. A direct measurement of this cross section with a neutron beam at this energy gave $\sigma_{\rm tot}(np \to d\pi^0) = (1.6 \pm 0.27)$ mb [18]. Alternatively, on the basis of isospin, $\sigma_{\rm tot}(pn \to d\pi^0) = \frac{1}{2}\sigma_T(pp \to d\pi^+) = (1.53 \pm 0.01)$ mb, where we have used values from the standard data compilation [19]. The agreement with our result is therefore very satisfactory.

5 Conclusions

We have here described the construction and application of a solid state telescope capable of measuring slow protons and deuterons in the ultra-high vacuum conditions pertaining at an internal-target station of a storage ring. The technique enables us not only to identify the particles but, also to measure their kinetic energies with 1% precision. Using the tracking capabilities of the set-up the angle of the spectator can be determined and the relative positions of the target and all detectors measured, such that geometrical uncertainties are minimised.

The combination of the silicon telescope with a magnetic analysis system for fast particles permits the identification of reactions on the neutron in the

13

deuterium target and the measurement of their absolute cross sections. The centre-of-mass energies in such reactions are well defined by the kinematics of the spectator proton and, in fact, the deuteron Fermi motion allows a scan over a wide range of energies while keeping the beam momentum fixed. Apart from the $pn \rightarrow d\pi^0$ test experiment reported here, the system has already been used to investigate near-threshold ω [3] and η [5] production from the neutron.

A further use of this technique is the monitoring of the luminosity in experiments at storage rings. The energy of a recoil deuteron detected near 90° determines very well the kinematics of elastic proton-deuteron scattering, thus fixing the luminosity in terms of the $pd \rightarrow pd$ differential cross section. This method was employed in the analysis of our $pn \rightarrow d\omega$ measurement [3] and other reactions at ANKE. With the current set-up it could not be used for the $pn \rightarrow d\pi^0$ measurement presented here. This geometric limitation can be overcome by an optimised positioning of the system within the redesigned vacuum chamber at ANKE. It is important to note that the telescope can also be used to evaluate the luminosity for pp reactions with a hydrogen target by measuring the low energy proton from pp elastic scattering near 90°.

Another application of the set-up is the measurement of the beam polarisation, which is becoming increasingly important in view of the number of polarisation measurements proposed at COSY [20]. It was proven, using the telescope described here, that it was possible to do this in parallel to data-taking without any harm to or restriction on the beam [21].

The experience gained in building and using the spectator counter system has been put to use in the design of second-generation silicon telescopes [22]. Putting four of these new telescopes even closer to the beam will increase the geometrical acceptance by a factor 40. Since all the detectors, especially the $65\,\mu$m layers, will be double-sided strip detectors, the angles of even low energy spectators will be measured to $\sigma(\theta) = \sigma(\phi) = 1° - 3°$. This means that the tracks from the extended target region of a polarised gas target could also be reconstructed. This will open the window to use polarised deuterium as a source for polarised proton-polarised neutron physics.

6 Acknowledgements

References

[1] R. Bilger et al., Nucl. Instr. Meth. A 457 (2001) 64.

[2] P. Moskal and T. Johansson, COSY proposal 100 (2001) (unpublished).

[3] S. Barsov et al., Eur. Phys. J. (*in press*),
http://de.arXiv.org/abs/nucl-ex/0305031

[4] I. Lehmann, PhD thesis, University of Cologne, 2003.

[5] N. Lang, IKP Annual Report 2003, Forschungszentrum Jülich;
A. Khoukaz, COSY proposal 94 (2000) (unpublished),
http://www.fz-juelich.de/ikp/anke/en/proposals.shtml .

[6] S. Barsov et al., Nucl. Instr. Meth. A 462/3 (2001) 364.

[7] G. Riepe and D. Protić, Nucl. Instr. Meth. A 226 (1984) 103.

[8] I. Lehmann, Diploma thesis, University of Cologne (2000);
Internal Report, Forschungszentrum Jülich: FZJ-IKP-IB-E2-1/2000;
http://www.fz-juelich.de/ikp/anke/en/theses.shtml .

[9] P.A. Schlosser et al., IEEE Trans. Nucl. Sci., vol. 21, no. 1 (1974) 658.

[10] J. F. Ziegler, J.P. Biersack, and U. Littmark, *The Stopping and Range of Ions in Solids*, Pergamon Press (N.Y., 1985); http://www.srim.org

[11] GEANT3, CERN Program Library W5013, CERN, 1993;
http://wwwinfo.cern.ch/asdoc/geant_html3/geantall.html

[12] V. Komarov et al., Phys. Lett. B 553 (2003) 179.

[13] V. Franco and R. J. Glauber, Phys. Rev. 142 (1966) 1195.

[14] E. Boschitz et al., Phys. Rev. C 6 (1972) 457.

[15] Yu. Uzikov, IKP Annual Report 2001, Forschungszentrum Jülich, p. 66; (private communication).

[16] E. Chiavassa et al., Phys. Lett. B 337 (1994) 192.

[17] PLUTO, A Monte Carlo simulation tool, GSI, 2000
http://www-hades.gsi.de/computing/pluto/html/PlutoIndex.html

[18] S. S. Wilson et al., Nucl. Phys. B 33 (1971) 253.

[19] R. A. Arndt et al., Phys. Rev. C 48 (1993) 1926;
http://gwdac.phys.gwu.edu/analysis/pd_analysis.html

[20] V. Komarov, COSY proposal 20 (1999) (unpublished),
A. Kacharava and F. Rathmann, COSY proposal 125 (2003) (unpublished),
http://www.fz-juelich.de/ikp/anke/en/proposals.shtml .

[21] S. Yaschenko et al., IKP Annual Report 2002, Forschungszentrum Jülich.

[22] R. Schleichert et al., IEEE Trans. Nucl. Sci., vol. 50, no. 3 (2003) 301;
R. Schleichert, COSY proposal 114 (2002) (unpublished),
http://www.fz-juelich.de/ikp/anke/en/proposals.shtml .